Life Sciences 239 (2019) 116903

Contents lists available at ScienceDirect

Life Sciences

journal homepage: www.elsevier.com/locate/lifescie

Mechanism of electrical remodeling of atrial myocytes and its influence on susceptibility to atrial fibrillation in diabetic rats

Lu Fu[a,b,1], Fang Rao[a,b,1], Feihong Lian[a,b], Hui Yang[a,b], Sujuan Kuang[a,b], Shulin Wu[a,b], Chunyu Deng[a,b,**], Yumei Xue[a,b,*]

[a] Department of Cardiology, Guangdong Cardiovascular Institute, Guangdong Provincial People's Hospital, Guangzhou, 510080, China
[b] Guangdong Provincial Key Laboratory of Clinical Pharmacology, Research Center of Medical Sciences, Guangdong Academy of Medical Sciences, Guangzhou, 510080, China

ARTICLE INFO

Keywords:
Diabetes
Atrial fibrillation
AF susceptibility
Electrical remodeling

ABSTRACT

Aims: To explore the atrial electrical remodeling and the susceptibility of atrial fibrillation (AF) in diabetic rats.
Materials and methods: Zucker diabetic fatty (ZDF) rats were chosen as diabetic animal model, and age-matched non-diabetic littermate Zucker lean (ZL) rats as control. AF susceptibility was determined by electrophysiological examination. The current density of I_{to}, I_{Kur} and $I_{Ca\text{-}L}$ were detected by whole-cell patch-clamp technique, and ion channel protein expression in atrial tissue and HL-1 cells treated with advanced glycation end products (AGE) was analyzed by western blotting.
Key findings: Diabetic rats had significantly enlarged left atria and evenly thickened ventricular walls, hypertrophied cells and interstitial fibrosis in atrial myocardium, increased AF susceptibility, and prolonged AF duration after atrial burst stimulation. Compared with atrial myocytes isolated from ZL controls, atrial myocytes isolated from ZDF rats had prolonged action potential duration, decreased absolute value of resting membrane potential level and current densities of I_{to}, I_{Kur} and $I_{Ca\text{-}L}$. The ion channel protein (Kv4.3, Kv1.5 and Cav1.2) expression in atrium tissue of ZDF rats and HL-1 cells treated with high concentration AGE were significantly down-regulated, compared with controls.
Significance: The atrial electrical remodeling induced by hyperglycemia contributed to the increased AF susceptibility in diabetic rats.

1. Introduction

Atrial fibrillation (AF), one of the most common tachyarrhythmia, is associated with cardiovascular mortality and morbidity [1,2]. Diabetes mellitus (DM) is a worldwild chronic disease, which is an independent risk factor for AF [3]. The incidence of AF in DM patients is nearly 40% higher than that of in normal people, and the mortality rate of DM patients with AF is 61% higher than that of simple DM patients [4,5].

Studies on patients and animal models of AF suggest that both electrical and structural remodeling of atria contribute to the occurrence and maintenance of AF. Atrial electrical remodeling during AF mainly includes shortening of atrial effective refractory period (ERP), atrial myocyte action potential duration (APD) and conduction disorder [6]. Abnormal glucose metabolism triggers cardiac autonomic dysfunction, changes in myocardial pathological and oxidative stress, leading to atrial electrical and structural remodeling, which promotes AF occurrence [6]. However, the electrical remodeling mechanisms associated with diabetes and AF remains unclear, with most studies on diabetics focusing on ventricular and few on atrium. Cardiac calcium regulation is impaired in diabetics [6]. Previous studies of type 1 diabetes mellitus (T1DM) model animals showed that Ca^{2+} regulation of T1DM atrial myocytes was impaired, APD of atrial myocytes was significantly prolonged, while changes in cell transient outward K^+ current (I_{to}) and L-type Ca^{2+} channels ($I_{Ca\text{-}L}$) current density were inconsistent [7–9]. There are limited studies on ultrafast delayed rectifier K^+ current (I_{Kur}) in cardiomyocytes of diabetic model animals and on

* Corresponding author. Department of Cardiology, Guangdong Cardiovascular Institute, Guangdong Provincial People's Hospital, Guangdong Academy of Medical Sciences, Guangzhou, 510080, China.
** Corresponding author. Guangdong Provincial Key Laboratory of Clinical Pharmacology, Research Center of Medical Sciences, Guangdong Academy of Medical Sciences, Guangzhou, 510080, China.
E-mail addresses: chunyudeng@126.com (C. Deng), xymgdci@163.com (Y. Xue).
[1] Lu Fu and Fang Rao (MD) contributed equally to this work.

https://doi.org/10.1016/j.lfs.2019.116903
Received 24 June 2019; Received in revised form 14 September 2019; Accepted 22 September 2019
Available online 19 October 2019

electrical remodeling in type 2 diabetes mellitus (T2DM) model animals. In catheter ablation of paroxysmal AF, patients with DM have longer biventricular activation time, lower atrial voltage, and higher recurrence rate (18.8 ± 6.4 months follow-up) [10].

The present study aimed to investigate electrical remodeling mechanisms in atrial myocytes of diabetic rats. Zucker diabetic fatty (ZDF) rats and Zuker lean (ZL) rats were selected as diabetic model and controls, respectively. AF susceptibility was tested, and the APD, ion channel current density and related protein expression levels of atrial myocytes were assessed. Mouse atrial HL-1 cells [11] treated with advanced glycation end products (AGE) [12,13] were used to explore the related mechanisms of atrial electrical remodeling in DM.

2. Materials and Methods

2.1. Study design and preparation of the T2DM rat model

The T2DM model was established in ZDF rats. SPF-class 7-week-old male ZDF rats and ZL rats were purchased from Beijing Vital River Laboratory Animal Technology Co., Ltd. (production license: SCXK [high] 2012–0001). Rats in both groups were fed with Purina #5008 feed. Body weight and metabolic indicators were measured in 20-week-old rats. Cardiac echocardiography, atrial histopathological examination, electrophysiological examination at the body level, detection of ion current density in atrial myocytes and ion channel protein expression of atrial tissue were performed in 20-week-old rats. All animal experiments were carried out in accordance with the requirements of the NIH Laboratory Animal Protection and Use Guidelines (8th, Edition, National Research Council, 2011). All animal experiments were approved by the animal experiment ethical review committee of Guangdong Provincial People's Hospital (Guangdong Academy of Medical Sciences) (No.GDREC201208A).

2.2. Body weight, blood biochemical index, pathological and echocardiographic examination

The body weight and blood biochemical index, including random blood glucose (RBG), cholesterol (CHOL), triglycerides (TG), high-density lipoprotein (HDL), low-density lipoprotein (LDL), blood urea nitrogen (BUN), creatinine (Cre), and non-esterified fatty acid (NEFA), were measured on 10 in each group of 20-week-old rats. Cardiac echocardiography was performed via the Vevo 2100 Color Doppler Small Animal Ultrasound Scanner (Visual Sonic) to determine the left atrial area (LAA) and left ventricular end-diastolic anterior wall thickness (LVAWd), left ventricular end-diastolic posterior wall thickness (LVPWd), left ventricular end-diastolic internal dimension (LVIDd), left ventricular diastolic volume (LVd), left ventricular end-systolic anterior wall thickness (LVAWs), left ventricular end-systolic posterior wall thickness (LVPWs), left ventricular end-systolic internal dimension (LVIDs), left ventricular systolic volume (LVs), stroke volume (SV), left ventricular ejection fraction (LVEF). For atrial histopathological examination, atrium tissue was embedded in 10% neutral formalin for 24 h, and serially sliced by a paraffin microtome, each having a thickness of 3.5 μm for Hematoxylin-eosin staining (HE staining) and Masson's trichrome staining (Masson staining).

2.3. Detection of susceptibility to AF and related electrophysiological properties

After anesthesia by intraperitoneal injection of 3% pentobarbital sodium (30 mg/kg), the experimental rat was placed in a supine position on a test bench. The limb lead electrode was placed under the skin of the rat's limbs. A midline incision was made in the neck to fully expose the internal jugular vein for insertion of a sheath tube. The multi-conducting physiological recorder, lead electrode, and Labscribe data acquisition software were connected. Under the guidance of intracardiac and limb lead electrocardiography, the electrode catheter was localized to the right atrium. The sinus cycle length (SCL) was determined by the mean of 10 consecutive RR intervals in lead II, and the P wave duration (PWD) was measured.

To measure pacing threshold, the pace pulse width was set to 1 ms, and the pacing frequency was 10 times/min faster than the basal heart rate. When recording a sustained atrial capture, suggesting that the electrode reaches the atria and the pacing was good, the electrode was fixed. For sinus node recovery time (SNRT) measurement, continuous single stimulation mode was used, basic cycle length (BCL) was set to 100 ms, stimulation output was twice the pacing threshold, and stimulation pulse width was 1 ms of 30 s continuous pacing. SNRT was defined as the time from the last pacing pulse signal to the first recovery of the sinus P wave origin, and the corrected sinus node recovery time (CSNRT) was calculated by subtracting SCL from SNRT. For induction of AF, atrial burst stimulation, BCL 20 ms, output 6 V, pulse width 2.5 ms, and pacing time 30 s, was repeated 10 times. Successful induction of AF was defined as irregular electrical activity of the atrium lasting for more than 1 s, with limb ECG showing P wave disappearance with replacement by f waves of different sizes, uneven intervals and different forms with variable RR interval, and intracavity electrogram showing irregular tremors. The AF induction rate (AFIR) and the mean duration of AF (MDAF) of each group were recorded. MDAF was calculated as the mean value of AF duration from onset to self-termination after 10-time induction.

2.4. Whole-cell patch-clamp studies on rat atrial myocyte

The Langendorff constant-flow perfusion device was used to perfuse the isolated hearts of 20-week-old rats, and the rat atrial myocytes were isolated. The perfusate (2.75 g MEM medium, 0.65 g HELP-Na, 0.225 g $NaHCO_3$, 250 ml distilled water, and pH 7.35 with NaOH) and enzymatic hydrolysate (40 ml perfusion solution + 0.04 g bovine serum albumin (BSA) + 0.02 g collagenase) were pre-heated. Rat atrial myocytes were collected in tube containing KB solution (mM): 50 K-Glutamate, 20 KOH, 40 KCl, 20 KH_2PO_4, 20 Taurine, 10 Glucose·H_2O, 3 $MgCl_2$·$6H_2O$, 0.5 EGTA, 10 HEPES, and pH 7.4 with KOH.

Whole-cell patch clamp with an Axopatch 200B amplifier (Axon Instruments) was used to record relevant indicators for single atrial myocyte. When recording action potential, the bath solution contained (mmol/l): 145 NaCl, 4 KCl, 1 $MgCl_2$, 1.8 $CaCl_2$, 10 HEPES, and pH 7.4 with NaOH. The pipette solution contained (mmol/l): 120 K-aspartate, 25 KCl, 1 $MgCl_2$, 10 EGTA, 2 Na_2 phosphocreatine, 4 Na_2ATP, 2 NaGTP, 5 HEPES, and pH 7.2 with KOH. To study I_{to} and I_{Kur}, the cells were superfused with bath solution containing (mmol/l): 140 NaCl, 4 KCl, 1 $MgCl_2$, 10 HEPES, 2 $CaCl_2$, 10 glucose, 0.5 $CdCl_2$, and pH 7.4 titrated with NaOH. The pipette solution contained (mmol/l): 90 potassium aspartate, 20 KCl, 10 HEPES, 1 $MgCl_2$, 5 Na_2ATP, 5 EGTA, and pH 7.2 with KOH. To study $I_{Ca\text{-}L}$, the pipette was filled with a high Cs^+ solution consisted of (mmol/l): 100 CsCl, 20 TEA-Cl, 5 Na_2ATP, 0.4 Na_2GTP, 10 EGTA, 10 HEPES, and pH 7.2 with Tris. The bath solution consisted of (mmol/l): 140 TEA-Cl, 5 $CaCl_2$, 2 $MgCl_2$, 10 HEPES, 10 Glucose, and pH 7.4 with CsOH.

Data were collected once the current amplitude had been stabilized. Current signals were filtered at 1 kHz bandwidth and then sampled at 10 kHz and stored on the hard disk of an IBM-AT-compatible computer using an on-line data acquisition program (pCLAMP 8, Axon). SigmaPlot 10.0 was used for curve fitting and plot ion channel current density, recovery, inactivation curve, APD curve fitting, calculation of action of repolarization 50%, 90% Potential time course (APD50, APD90), resting membrane potential (RMP), peak action potential (PAP), and action potential amplitude (APA).

All average data are expressed in terms of current density due to differences in cell size. Current density (pA/pF) = current intensity/capacitance.

The voltage dependence of ion channel current (I_{to} and $I_{Ca\text{-}L}$)

activation was determined from the g/g_{max} ratio, where g is the conductance and g_{max} is the maximum g value, by using the I–V relation of the related iron channel. The relationship between g/g_{max} and membrane potential was fitted to the Boltzmann equation: $g/g_{max} = 1/\{1 + \exp[(V_{0.5} - V)/S]\}$, where $V_{0.5}$ is the estimated half-maximum activation voltage, V is the test potential, and S is the slope factor. Inactivation variability (I/I_{max}) was determined as ion channel current at a given prepulse potential divided by the maximum ion channel current in the absence of a prepulse. The inactivation curve was fitted to a Boltzmann function with the following equation: $I/I_{max} = 1/\{1 + \exp[(V–V_{0.5})/S]\}$, where $V_{0.5}$ is the estimated half-maximum inactivation voltage, V is the prepulse potential, and S is the slope factor. Time-dependent recovery of ion channel current (I_{to} and $I_{Ca\text{-}L}$) from inactivation was studied using a paired-pulse protocol (P1, P2). Current during P2 (I2) relative to the current during P1 (I1) was plotted as a function of the P1–P2 interval.

2.5. Western blotting analysis

Western blot was used to detect the expression of protein Kv4.3, Kv1.5 and Cav1.2 in rat atrial tissue and HL-1 cells treated with or without AGEs (Biovision, USA) (50 μg/ml, 100 μg/ml, and 200 μg/ml) for 48h. Proteins of atrial tissue and HL-1 cells were extracted as previously described [14,15]. An equal amount of protein was loaded onto a 10% or 15% sodium dodecyl sulfate (SDS) denaturing polyacrylamide gel, separated by electrophoresis, transferred onto polyvinylidene fluoride (PVDF) (Merck Millipore, USA), incubated with the specific primary antibody overnight at 4 °C, then washed and subsequently incubated with the secondary antibody for 1 h at room temperature or 2 h at 4 °C. Rabbit-derived Kv1.5, Kv4.3 and Cav1.2 polyclonal antibodies were purchased from Alomone, Israel. Rabbit-derived glyceraldehyde-3- phosphate dehydrogenase (GAPDH) polyclonal antibody was purchased from Santa Cruz, USA. HRP-labeled secondary antibody (goat anti-rabbit) was purchased from Abcam, USA. Protein was visualized using enhanced chemiluminescence. Protein levels were expressed relative to levels of GAPDH. The Image J Analysis Imaging System calculated the gray value of each strip and the images were plotted by the GraphPad Prism system.

2.6. Statistical analysis

All data are expressed as mean ± standard error of the mean (SEM) and were analyzed using Graphpad PRISM 3.0 (Graphpad, San Diego, CA, USA) or Clampfit (Axon). Paired and/or unpaired Student's t-test was used as appropriate to evaluate the statistical significance of differences between two group means. Categorical variables are presented as percentages. A two-tailed $p < 0.05$ was considered statistically significant.

3. Results

3.1. Establishment of type 2 diabetes model and pathological changes of atrial tissue

ZDF rats of 20-week-old showed significant increases in RBG, CHOL, TG, HDL, LDL, BUN, and NEFA ($p < 0.05$ or $p < 0.01$ vs. ZL) as compared with ZL rats of the same age, except for Cre (Fig. 1). LAA was significantly increased in ZDF rats as compared with ZL rats ($p < 0.01$ vs. ZL). LVAWd, LVAWs, LVPWd, LVPWs, LVIDd, LVIDs and LVEF were increased ($p < 0.05$ or $p < 0.01$ vs. ZL), while LVd and LVs were decreased ($p < 0.05$ or $p < 0.01$ vs. ZL). These results indicated left atrial enlargement and left ventricular hypertrophy in ZDF rats (Table 1, Fig. 2).

Immunohistochemical staining suggested that the cardiomyocytes of ZDF rats were hypertrophied, arranged disorderly, with myocardial fibrosis presented in the myocardial interstitial (Fig. 3).

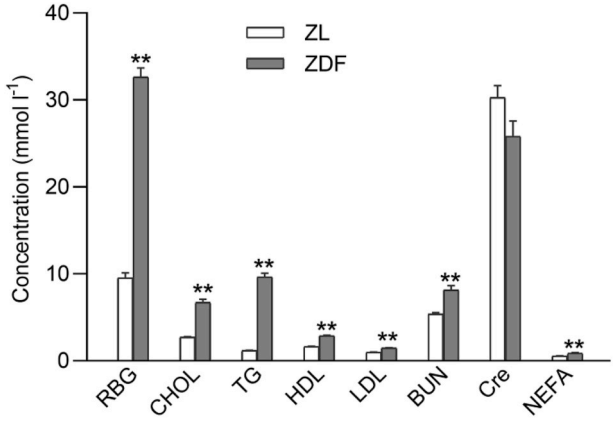

Fig. 1. Blood biochemical indexes of ZL and ZDF rats. Data are presented as mean ± SEM; **p < 0.01 vs. ZL. RBG: random blood glucose; CHOL: cholesterol; TG: triglycerides; HDL: high-density lipoprotein; LDL: low-density lipoprotein; BUN: blood urea nitrogen; Cre: creatinine; NEFA: non-esterified fatty acid.

Table 1
Echocardiographic parameters of the two groups of rats.

	ZL (n = 10)	ZDF (n = 10)
LAA(mm^2)	16.82 ± 1.59	20.04 ± 1.98**
LVAWd(mm)	1.76 ± 0.15	2.18 ± 0.10*
LVPWd(mm)	1.71 ± 0.06	2.19 ± 0.12*
LVIDd(mm)	7.73 ± 0.16	7.08 ± 0.14**
LVd(μL)	321.51 ± 14.86	263.58 ± 12.16*
LVAWs(mm)	2.52 ± 0.08	3.17 ± 0.09**
LVPWs(mm)	2.51 ± 0.05	3.12 ± 0.09**
LVIDs(mm)	5.25 ± 0.16	4.34 ± 0.12**
LVs(μL)	134.53 ± 9.61	86.08 ± 5.97**
SV(mm)	186.98 ± 7.16	177.50 ± 7.72
LVEF(%)	58.50 ± 1.38	67.52 ± 1.20**

Data are presented as mean ± SEM; *p < 0.05 vs. ZL, **p < 0.01 vs. ZL. LAA: left atrial area; LVAWd: left ventricular end-diastolic anterior wall thickness; LVPWd: left ventricular end-diastolic posterior wall thickness; LVIDd: left ventricular end-diastolic internal dimension; LVd: left ventricular diastolic volume; LVAWs: left ventricular end-systolic anterior wall thickness; LVPWs: left ventricular end-systolic posterior wall thickness; LVIDs: left ventricular end-systolic internal dimension; LVs: left ventricular systolic volume; SV: stroke volume; LVEF: left ventricular ejection fraction.

3.2. Susceptibility to atrial fibrillation in diabetic rats

Compared with the control group, diabetic rats had a higher rate of AF (77.1% vs. 12.5%, $p < 0.01$) after atrial burst stimulation, and significantly longer MDAF (66.83 ± 26.18 s vs. 2.64 ± 1.36 s, $p < 0.05$). Electrocardiographic PWD (47.00 ± 1.97 ms vs. 40.88 ± 0.88 ms, $p < 0.05$), SCL (239.43 ± 15.25 ms vs. 190.25 ± 11.12 ms, $p < 0.05$), SNRT (525.43 ± 69.11 ms vs. 259.38 ± 18.83 ms, $p < 0.01$) and CSNRT (286.00 ± 69.17 ms vs. 69.13 ± 18.61 ms, $p < 0.05$) in diabetic rats were significantly longer than those in control rats (Fig. 4).

3.3. Changes in APD of atrial myocytes in diabetic rats

Compared with atrial myocytes isolated from ZL control rat, the APD of diabetic rat atrial myocytes was significantly prolonged, with higher APD_{50} ($p < 0.01$) and APD_{90} ($p < 0.01$), and RMP level was lower ($p < 0.05$). There was no significant difference in APA between the two groups ($p > 0.05$) (Fig. 5).

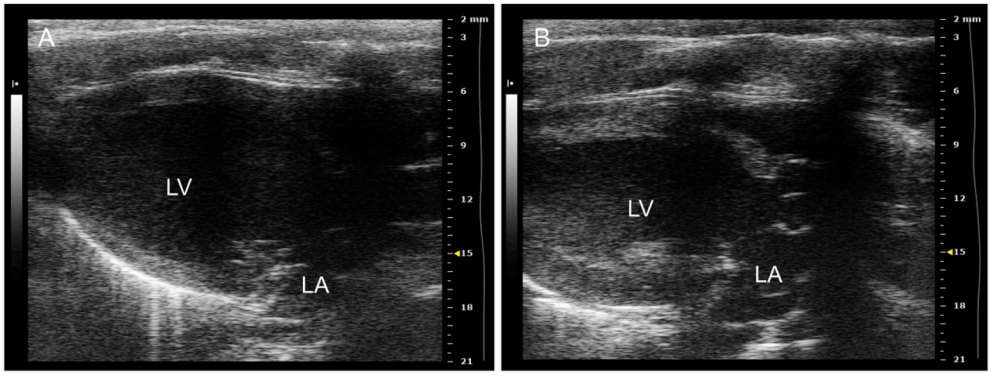

Fig. 2. The images of M-mode echocardiography for the ZL (A) and ZDF (B) rat. LV: left ventricle; LA: left atrium.

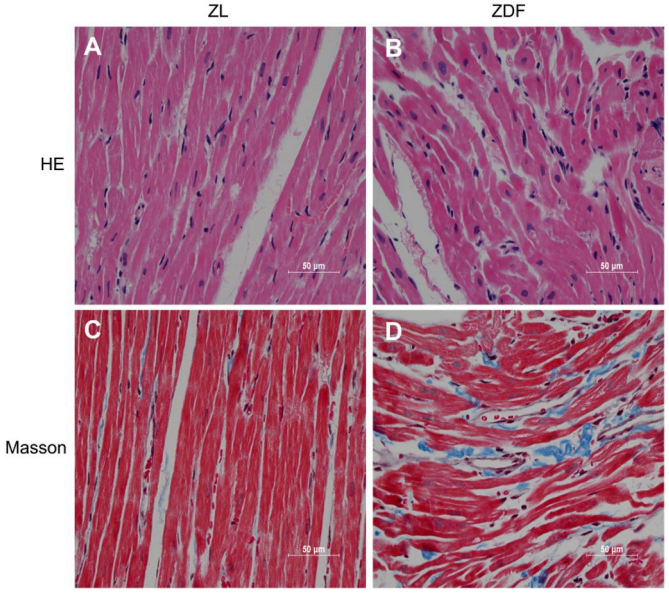

Fig. 3. HE staining and Masson staining of ZL atrial tissue (A, C) and ZDF atrial tissue (B, D).

3.4. Changes in I_{to} and I_{kur} of atrial myocytes and related protein expression of atrial tissue in diabetic rats

I_{to} current density in diabetic rat atrial myocytes was significantly lower than that in the control, as shown in Fig. 6 panel A. However, there were no significant differences in the kinetics of I_{to} (Fig. 6 panel B activation/inactivation curve). The expression level of the protein Kv4.3 in diabetic atrial tissue was significantly down-regulated ($p < 0.01$, Fig. 6 panel D).

Current density of I_{Kur} in atrial myocytes of diabetic rats was also significantly lower than that in controls ($p < 0.05$, Fig. 7 panel A). And the expression of protein Kv1.5 in diabetic atrial tissue was significantly down-regulated, compared with control ($p < 0.05$, Fig. 7 panel B).

3.5. Changes in $I_{Ca\text{-}L}$ of atrial myocytes and Cav1.2 protein expression of atrial tissue in diabetic rats

Current density of $I_{Ca\text{-}L}$ in the atrial myocytes of diabetic rats was significantly lower than that of controls ($p < 0.05$ or $p < 0.01$) (Fig. 8 panel A), while the kinetics of $I_{Ca\text{-}L}$ (Fig. 8 panel B) remained statistically similar to that of controls. Compared with the control group, the protein expression level of Cav1.2 in the diabetic atrial tissue was significantly lower ($p < 0.01$, Fig. 8 panel D).

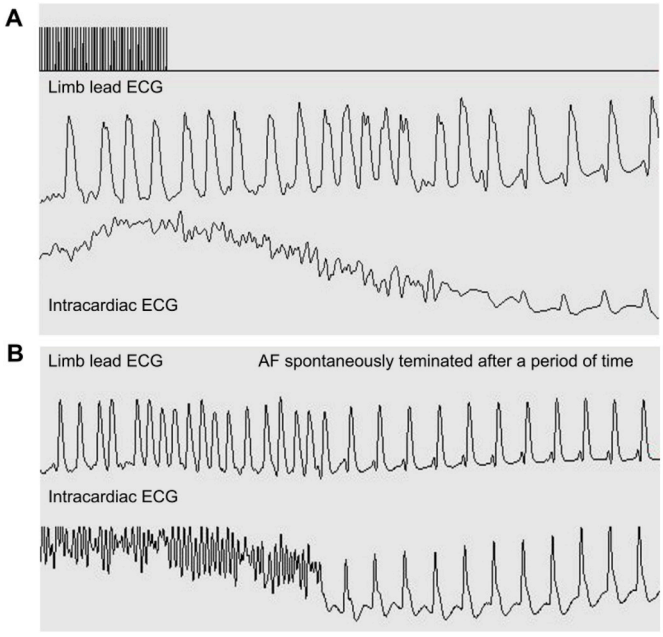

C

	ZL (n = 8)	ZDF (n = 7)
AFIR（%）	12.5	77.1**
MDAF（s）	2.64 ± 1.36	66.83 ± 26.18*
PWD（ms）	40.88 ± 0.88	47.00 ± 1.97*
SCL（ms）	190.25 ± 11.12	239.43 ± 15.25*
SNRT（ms）	259.38 ± 18.83	525.43 ± 69.11**
CSNRT（ms）	69.13 ± 18.61	286.00 ± 69.17*

Fig. 4. Susceptibility to AF and related electrophysiological parameters of ZL and ZDF rats. A: induction of short-array AF by atrial burst stimulation, and then return to sinus rhythm; B: limb lead and intracavitary electrocardiogram of AF converted to sinus rhythm; C: electrophysiological examination parameters and AF induction in the two groups. Data are presented as mean ± SEM; *p < 0.05 vs. ZL, **p < 0.01 vs. ZL. AFIR: AF induction rate; MDAF: mean duration of AF; PWD: P wave duration; SCL: sinus cycle length; SNRT: sinus node recovery time; CSNRT: corrected sinus node recovery time.

3.6. Effect of AGE on the expression of ion channel protein Kv4.3, Kv1.5 and Cav1.2 in HL-1 cells

As shown in Fig. 9, after treated with different concentrations of AGE for 48 h, the expression level of ion channel protein in HL-1 cells

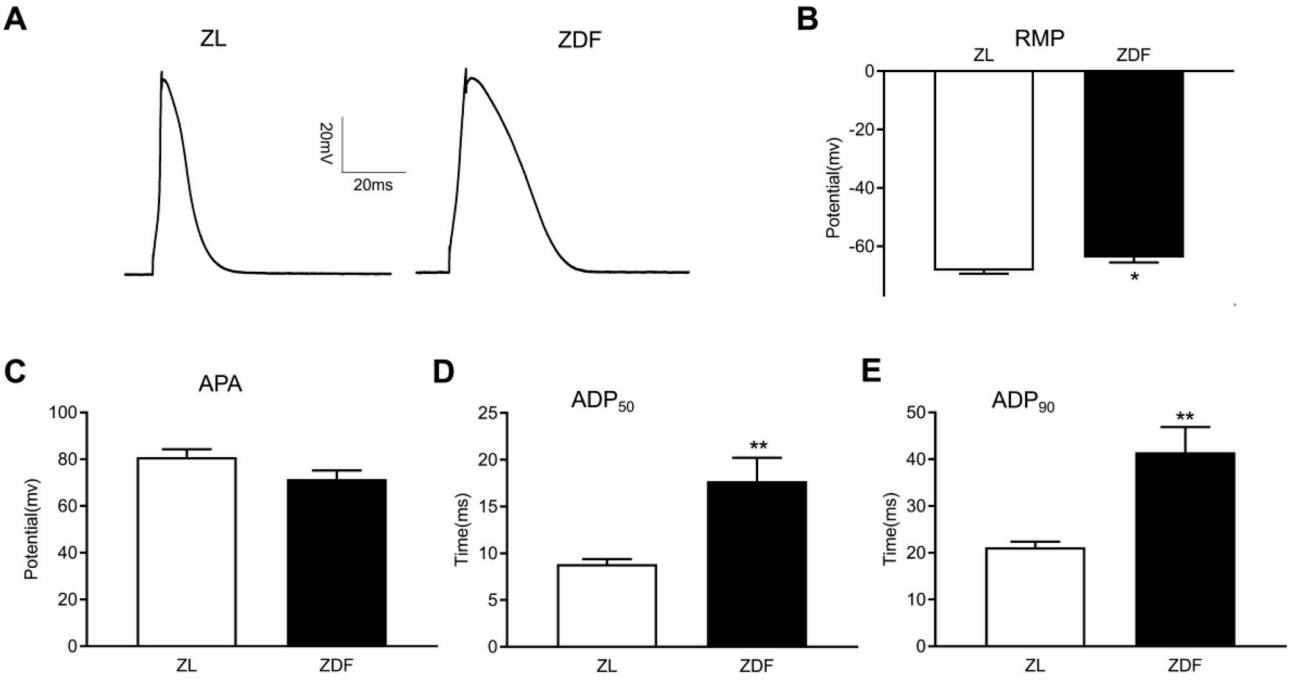

Fig. 5. APD of atrial myocytes isolated from ZL and ZDF rats. A: Representative action potential were recorded in representative isolated ZL and ZDF atrial myocytes with a perforated patch configuration at 2 Hz. Resting potential levels (B), APA (C), APD_{50} (D) and APD_{90} (E) of atrial myocytes were calculated. n = 13 atrial myocytes/2 ZL rats, n = 14 atrial myocytes/3 ZDF rats. Data are presented as mean ± SEM; *p < 0.05 vs. ZL, **p < 0.01 vs. ZL. RMP: resting potential; APA: action potential amplitude; APD_{50}: action potential when repolarization 50% procedures; APD_{90}: action potential when repolarization 90% procedures.

changed significantly. HL-1 cells were treated with different concentration of AGE concentration (50, 100, and 200 μg/ml), cells treated with BSA as control. The expression levels of Kv4.3, Kv1.5 and Cav1.2 of HL-1 cells were significantly down-regulated after treated with high concentration of AGE (100, and 200 μg/ml).

3.7. Discussion/Conclusion

In this study, diabetic rats had significantly enlarged left atrial area, evenly thickened ventricular walls, and pathological changes in the atrial myocardium with hypertrophied myocardial cells and myocardial interstitial fibrosis. AF susceptibility in diabetic rats increased, with significantly prolonged duration of AF after atrial burst stimulation. Diabetic atrial myocytes had prolonged APD, and significantly decreased absolute value of RMP level. The current density of I_{to}, I_{Kur} and $I_{Ca\text{-}L}$ were significantly reduced in diabetic atrial myocytes, and ion channel protein (Kv4.3, Kv1.5 and Cav1.2) expression levels in diabetic atrial tissue were significantly reduced. Similarly, ion channel protein (Kv4.3, Kv1.5 and Cav1.2) expression levels in HL-1 cells were significantly down-regulated by high concentration AGE.

ZDF rats, selected as the diabetes model in this experiment, are characterized by obesity, hyperglycemia, hyperlipidemia, hyperinsulinemia and insulin resistance caused by genetic obesity gene mutations, and is close to the pathogenesis of human T2DM [16–18]. In this experiment, 20-week old ZDF rats showed significant increase in body weight and obviously abnormal metabolic indicators such as RBG and blood lipids. The overall structure and function of the atrium of ZDF rats were deteriorated, with left atrial enlargement and left ventricular hypertrophy. Pathological changes also had been observed in atrial tissue with hypertrophic disordered cardiomyocytes, fibrotic myocardial interstitia, deposited collagen fibers and enlarged intercellular spaces, indicating that the T2DM model was successfully constructed.

Diabetic rats had higher susceptibility to AF, with significantly prolonged duration of AF after burst stimulation, which is consistent with previous studies [19–21]. Previous studies mainly focused on T1DM animal models, such as alloxan-induced diabetic rabbits [9,22–25], and streptozotocin-induced diabetes model Wistar rats [19]. There are a few studies on T2DM model, such as Goto-Kakizaki rat [20] and ZDF rats [26]. The study in ZDF rats focused on structural but not electrical remodeling of diabetes-related atrium [26]. In the present study, ZDF rats were successfully used to establish T2DM models and assess diabetes-related atrial electrical remodeling.

Electrical and structural remodeling of the atria, are suggested to be the basic mechanism of AF triggering and maintenance. Atrial size is an important factor in the development of AF [6]. Left atrial diastolic dysfunction and myocardial lesions led to left atrial enlargement and abnormal atrial electrophysiological properties such as changes in conductivity and refractory period [6]. In this study, the LAA of diabetic rats was significantly larger than that of controls, suggesting the possibility that enlarged LAA played a role in the increased susceptibility to AF in diabetic rats. Atrial histopathological examination revealed fibrosis in the atria of diabetic rats, which is a major feature of atrial structural remodeling, leading to an uneven line of conduction and conduction velocity in the atrium, eventually bring in increased susceptibility to AF.

Consistent with previous studies of diabetic animal models, the APD of atrial myocytes in diabetic rats was prolonged in this study [19,23,27]. Prolongation of APD in diabetic ventricular myocytes had been well studied [28], but there were limited studies on APD of atrial myocytes. In STZ-induced diabetic rats, APD of atrial myocytes and ventricular myocytes were significantly delayed. In atrial myocardium, lengthening of APD was more pronounced at early rather than late phrase of repolarization [27]. The absolute value of resting potential level in diabetic rats was significantly lower, which might increase the frequency of early post-depolarization related to arrhythmia. The prolongation of APD of diabetic atrial myocytes is mainly caused by the repolarization of atrial myocytes, especially earlier phases of repolarization [27]. This study mainly explored the changes of current density of I_{to}, I_{Kur} and $I_{Ca\text{-}L}$ affecting early repolarization and the expression levels of related encoded proteins.

I_{to} constitutes the most in-depth study of myocardial ion channels in

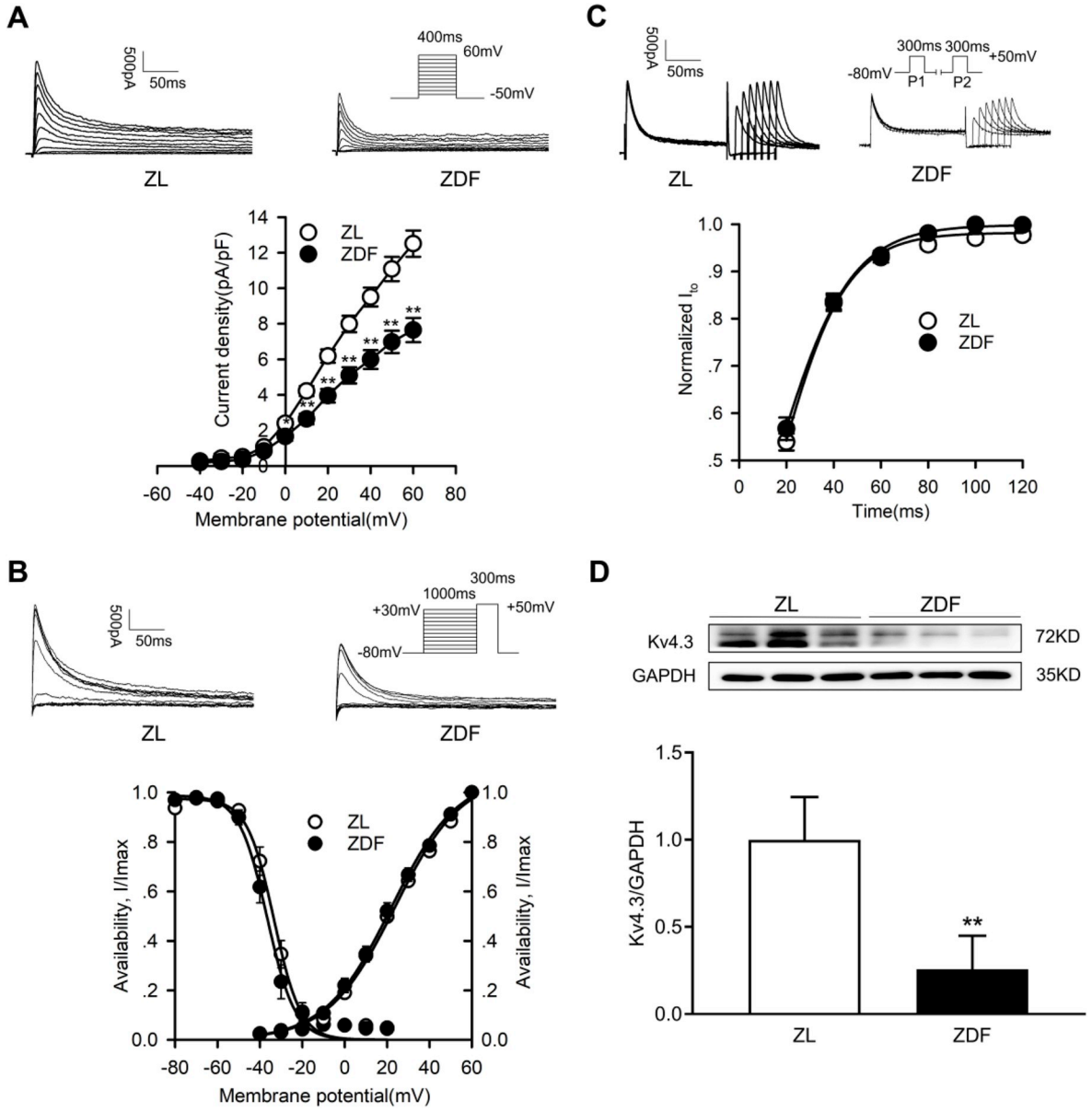

Fig. 6. Changes in I_{to} kinetics and related protein expression of atrial myocytes from atrial tissue in diabetic rats. A: I_{to} traces were recorded in a representative ZL and ZDF atrial myocyte using voltage steps of 400 ms steps to between −40 and 50 mV from −50 mV at 0.2 Hz; current-voltage relations of I_{to} density in ZL and ZDF atrial myocyte (n = 20 atrial myocytes/5 ZL rats, n = 16 atrial myocytes/4 ZDF rats). B: Representative current recordings were used to determine voltage dependence of I_{to} inactivation using 1000 ms prepulses from holding potential of −80 mV to 30 mV and to 50 mV for 300 ms, then back to −80 mV; mean values of voltage-dependent activation (n = 20 atrial myocytes/5 ZL rats, n = 16 atrial myocytes/4 ZDF rats) and inactivation relations for I_{to} in ZL and ZDF atrial myocytes. C: Recovery of I_{to} from inactivation in ZL and ZDF atrial myocyte using paired 300-ms pulses to 50 mV from a holding potential of −80 mV with variable intervals; mean data for time course of recovery of I_{to} from inactivation in ZL and ZDF atrial myocyte (n = 23 atrial myocytes/5 ZL rats, n = 15 atrial myocytes/4 ZDF rats). D: Levels of Kv4.3 protein expression in ZL and ZDF rat atrial tissue were assessed by western blot analysis using GAPDH as the internal control. Data are expressed as mean ± SEM. *p < 0.05 vs. ZL, and **p < 0.01 vs. ZL.

diabetic animal models. When the current density decreases, the cell repolarization is prolonged, as is APD. I_{to} of atrial myocytes in AF patients was reduced, and the expression levels of protein Kv4.3 and mRNA were significantly down-regulated [29–31]. I_{to} of ventricular myocytes in drug- or transgenic-induced T1DM animal models was also significantly reduced [21], while no change was found in atrial myocytes in diabetic rats induced by streptozotocin [7]. In this study, I_{to} of atrial myocytes isolated from T2DM model - ZDF rats was significantly decreased ($p < 0.05$), and the expression of Kv4.3 in diabetic atrial tissue was significantly down-regulated.

I_{Kur} is specifically presented in atrial myocytes, and mainly plays a role in the action potential 2-phase repolarization, and decreased I_{kur} will slow down repolarization finally prolonging APD [32]. In patients with AF, I_{Kur} current density was significantly reduced due to decreased expression of protein Kv1.5 [33], leading to prolonged APD and ERP in atrial myocytes [34–36]. Lack of I_{Kur} may prolong the atrial APD, increasing risk for early post-polarization, which is closely associated with AF [37]. There are few studies on I_{Kur} in diabetes. In this study, we found that, compared to controls, Kv1.5 protein expression in diabetic atrial tissue was significantly down-regulated, and current density of I_{Kur} in diabetic atrial myocytes was reduced.

$I_{Ca\text{-}L}$ is an inward current that plays a major role in the 2-stage plateau of the action potential and decreased $I_{Ca\text{-}L}$ leading to accelerated repolarization and shortened APD. $I_{Ca\text{-}L}$ in atrial myocytes of

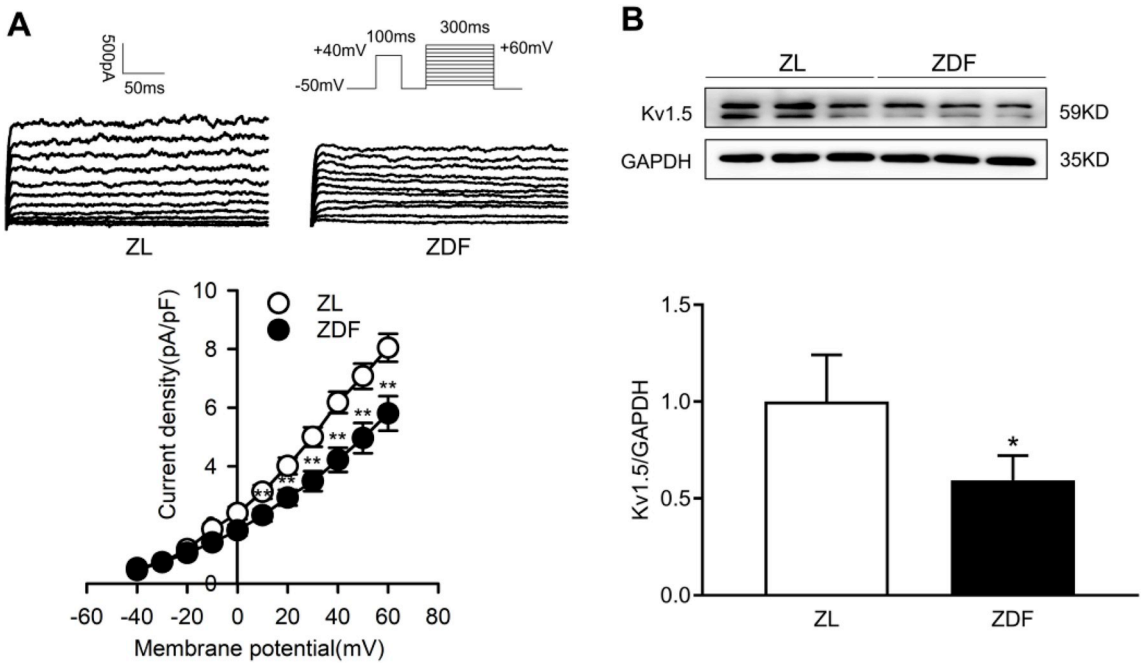

Fig. 7. Changes in I_{Kur} current density and related protein expression of atrial myocytes from atrial tissue in diabetic rats. A: I_{Kur} traces were recorded in a representative ZL and ZDF atrial myocyte by a 100 ms prepulse to +40 mV to inactivate I_{to}, followed by 300 ms test pulses between −40 and 60 mV after a 10 ms interval from −50 mV at 0.2 Hz; current-voltage relations of I_{Kur} density in ZL and ZDF atrial myocyte (n = 20 atrial myocytes/5 ZL rats, n = 16 atrial myocytes/4 ZDF rats). B: Levels of Kv1.5 protein expression in ZL and ZDF rat atrial tissue were assessed by western blot analysis using GAPDH as the internal control. Data are expressed as mean ± SEM. *p < 0.05 vs. ZL, and **p < 0.01 vs. ZL.

streptozotocin-induced diabetic rats was decreased, with decreased expression of Cav1.2 protein [8], while $I_{Ca\text{-}L}$ in atrial myocytes of alloxan-induced diabetic rabbits was increased [9]. The expression of Cav1.2 protein on the cell surface was also decreased in ventricular myocytes of diabetic rats [38,39], indicating that diabetes might have similar effects on ventricular and atrial ion channels. In this study, $I_{Ca\text{-}L}$ of diabetic atrial myocytes was significantly lower than that of controls, as well as the expression of Cav1.2 in diabetic atrial tissue.

Diabetic lesions cause changes in ionic currents of atrial myocytes, while ADP prolongation in atrial myocytes ultimately results from a combination of multiple ion channels. I_{to}, I_{Kur} and $I_{Ca\text{-}L}$ in atrial myocytes of diabetic rats in the study were significantly decreased, accompanied with the down-regulated expression levels of proteins Kv4.3, Kv1.5 and Cav1.2. Reduction of I_{to} and I_{Kur} leads to prolonged atrial repolarization, while decreased $I_{Ca\text{-}L}$ is associated with shortened repolarization time. Cardiac repolarization and refractory periods are determined by the balance of inward Ca^{2+} current and outward K^+ current. Compared with ventricular myocytes, atrial myocytes have more types and amounts of inward K^+ currents, such as I_{to}, I_{Kur}, and I_{Ks}. It was speculated that, multiple changes in ion channel currents were observed in diabetic atrial myocytes, APD prolongation induced by I_{to} and I_{Kur} reduction is greater than APD shortening induced by $I_{Ca\text{-}L}$ reduction, which ultimately leads to APD prolongation. APD prolongation might lead to AF by mediating multi-source atrial tachycardia [40].

Diabetes is characterized by chronic hyperglycemia which facilitates the irreversible formation of advanced glycation end products (AGEs), leading to the development of diabetic complication [12,13]. So in the present study, diabetic atrial myocyte model was established by HL-1 cells treated with AGE. We found that the expression levels of the ion channel-encoding proteins Kv4.3, Kv1.5 and Cav1.2 in HL-1 cells were significantly down-regulated when treated with AGE, further indicating that hyperglycemia might directly affect ion channel currents in atrial myocytes, thereby leading to atrial electrical remodeling, which is related to increased AF susceptibility.

3.8. Limitations

This study has several limitations. Only preliminary research was conducted on the effects of some ion channels on the action potential of atrial cells; however, APD is affected by the interaction of multiple ion channels, which warrants further research as do the signal-mediated pathways for atrial electrical and structural remodeling in diabetic rats and the determination of the ion channel current density of atrial myocytes after treated with AGE.

4. Conclusion

Diabetic rats showed evidence of atrial structural remodeling, i.e., left atrial enlargement and cardiac fibrosis, increased susceptibility to AF, significantly prolonged APD and decreased absolute value of RMP level in atrial myocytes. I_{to}, I_{Kur} and $I_{Ca\text{-}L}$ were significantly reduced in diabetic atrial myocytes, and ion channel protein (Kv4.3, Kv1.5 and Cav1.2) expression levels were also significantly down-regulated. Likewise, ion channel protein (Kv4.3, Kv1.5 and Cav1.2) expression levels in HL-1 cells were significantly down-regulated by high concentration AGE.

Author contributions

Lu Fu, Yumei Xue, Chunyu Deng, Fang Rao, Hui Yang and Shu-Lin Wu contributed to the conception and design of the research. Lu Fu, Chunyu Deng, and Fei-Hong Lian analyzed data generated in this study. Lu Fu, Fei-Hong Lian, Hui Yang, and Su-Juan Kuang performed the experiments described in this study. Lu Fu, Yumei Xue, Chunyu Deng, and Fang Rao interpreted the results of the experiments. Lu Fu, and Hui Yang prepared the figures and drafted the manuscript. Lu Fu, Chunyu Deng, Yumei Xue and Fang Rao edited and revised the manuscript. All authors read and approved the final version of the manuscript.

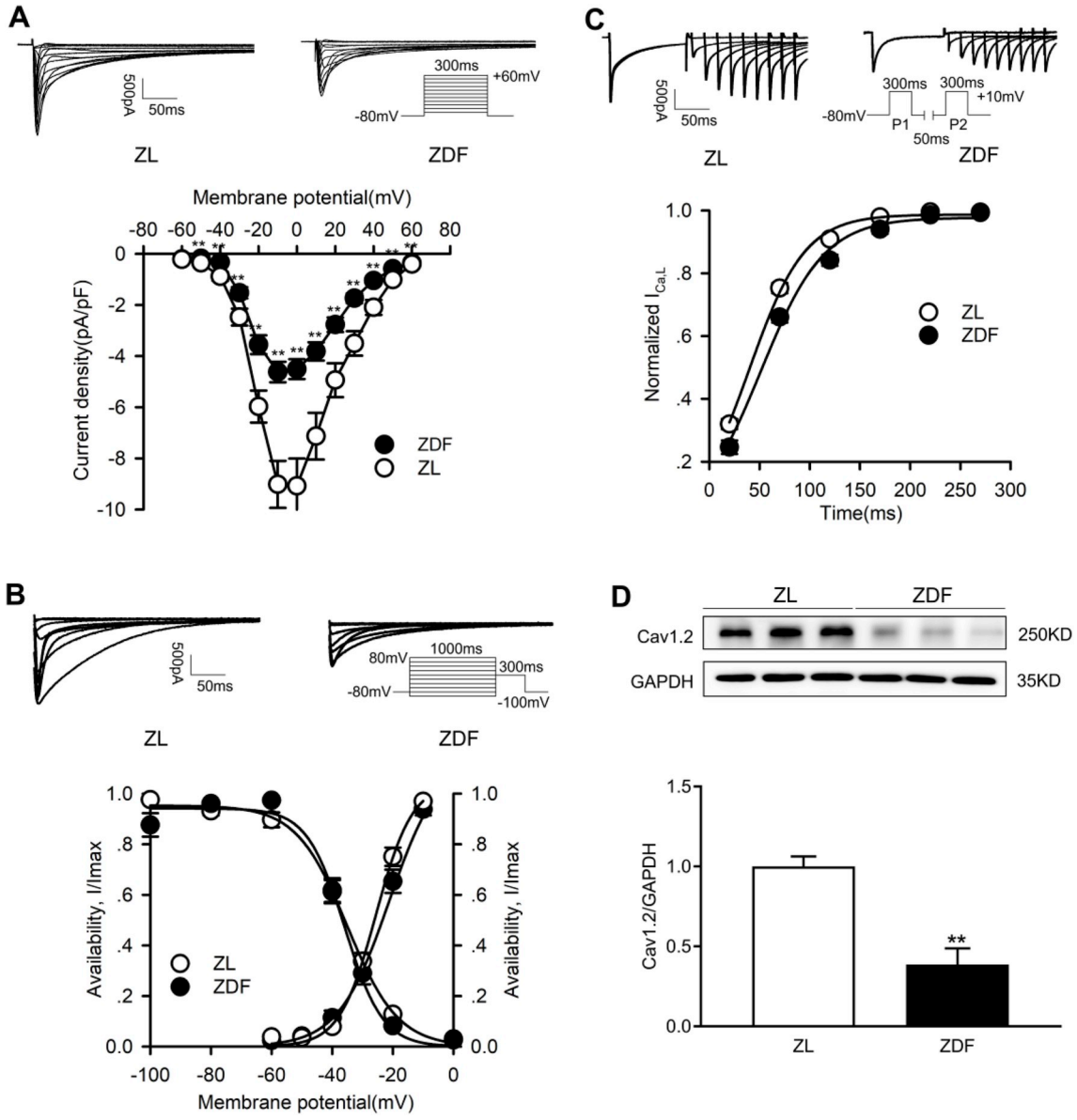

Fig. 8. Changes in $I_{Ca\text{-}L}$ kinetics and related protein expression of atrial myocytes from atrial tissue in diabetic rats. A: Representative $I_{Ca\text{-}L}$ traces were recorded using voltage steps of 300 ms steps to between −60 and 60 mV from the holding potential −80 mV at 0.2 Hz in a ZL atrial myocyte, and ZDF atrial myocyte; current-voltage relations of $I_{Ca\text{-}L}$ density in ZL and ZDF atrial myocytes (n = 21 atrial myocytes/5 ZL rats, n = 19 atrial myocytes/4 ZDF rats). B: Representative current recordings were used to determine voltage dependence of $I_{Ca\text{-}L}$ inactivation using 1000 ms prepulses from holding potential of −80 mV to between −100 and 80 mV and back to 0 mV for 300 ms, then subjected to −80 mV; mean values of voltage-dependent activation (n = 21 atrial myocytes/5 ZL rats, n = 19 atrial myocytes/4 ZDF rats) and inactivation (n = 23 atrial myocytes/5 ZL rats, n = 20 atrial myocytes/4 ZDF rats) relations for $I_{Ca\text{-}L}$ in ZL and ZDF atrial myocytes. C: Recovery of $I_{Ca\text{-}L}$ from inactivation using paired 300-ms pulses to 10 mV from a holding potential of −80 mV with 50-ms intervals in a ZL atrial myocyte, and ZDF atrial myocyte; mean data for time course of recovery of $I_{Ca\text{-}L}$ from inactivation in ZL and ZDF atrial myocyte (n = 21 atrial myocytes/9 ZL rats, n = 22 atrial myocytes/4 ZDF rats). D: Levels of Cav1.2 protein expression in ZL and ZDF rat atrial tissue were assessed by western blot analysis using GAPDH as the internal control. Data are expressed as mean ± SEM. *p < 0.05 vs. ZL, and **p < 0.01 vs. ZL.

Statement of ethics

All animal experiments were carried out in accordance with the requirements of the NIH Laboratory Animal Protection and Use Guidelines (8th, Edition, National Research Council, 2011). All animal experiments were approved by the animal experiment ethical review committee of Guangdong Provincial People's Hospital (Guangdong Academy of Medical Sciences) (Batch number: No.GDREC201208A).

Funding sources

This study was supported by a grant from the National Natural Science Foundation of China (No. 81870254, No.81470440, No.81670314).

Declaration of competing interest

The authors have no conflicts of interest to declare.

Acknowledgement

First of all, I would like to show my deepest gratitude to my supervisor, Dr. Yumei Xue, who has provided me with valuable guidance in every stage of the writing of this thesis. Secondly, I will thank Dr.

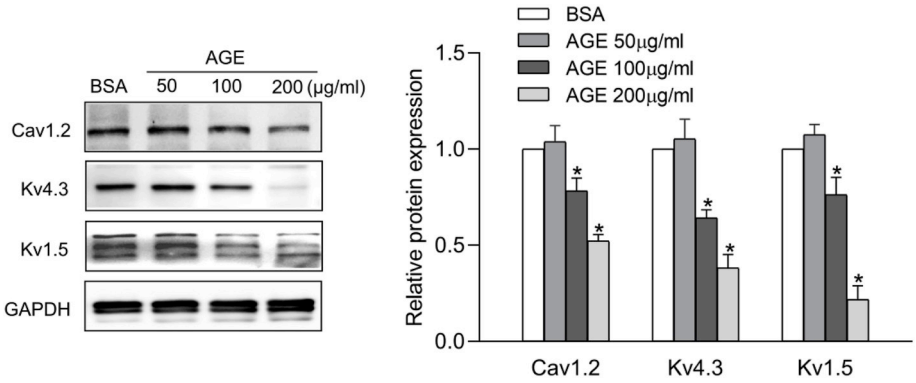

Fig. 9. Expression levels of ion channel protein in HL-1 cells treated with different concentrations of AGE for 48 h. Data are expressed as mean ± SEM, *p < 0.05 vs. HL-1 cells treated with BSA.

Chunyu Deng and Dr. Fang Rao for their great help in laboratory procedure, offered references, and the writing. Finally, I would like to thank Guangdong Cardiovascular Institute, Guangdong Provincial People's Hospital, Guangdong Provincial Key Laboratory of Clinical Pharmacology, Research Center of Medical Sciences, and Guangdong Academy of Medical Sciences for providing a platform for me to grow.

References

[1] J. Ball, M.J. Carrington, J.J. McMurray, S. Stewart, Atrial fibrillation: profile and burden of an evolving epidemic in the 21st century, Int. J. Cardiol. 167 (2013) 1807–1824.
[2] F. Rahman, G.F. Kwan, E.J. Benjamin, Global epidemiology of atrial fibrillation, Nat. Rev. Cardiol. 11 (2014) 639–654.
[3] Q. Zhang, T. Liu, C.Y. Ng, G. Li, Diabetes mellitus and atrial remodeling: mechanisms and potential upstream therapies, Cardiovasc Ther 32 (2014) 233–241.
[4] R.R. Huxley, K.B. Filion, S. Konety, A. Alonso, Meta-analysis of cohort and case-control studies of type 2 diabetes mellitus and risk of atrial fibrillation, Am. J. Cardiol. 108 (2011) 56–62.
[5] X. Du, T. Ninomiya, B. de Galan, E. Abadir, J. Chalmers, A. Pillai, et al., Risks of cardiovascular events and effects of routine blood pressure lowering among patients with type 2 diabetes and atrial fibrillation: results of the ADVANCE study, Eur. Heart J. 30 (2009) 1128–1135.
[6] J. Andrade, P. Khairy, D. Dobrev, S. Nattel, The clinical profile and pathophysiology of atrial fibrillation: relationships among clinical features, epidemiology, and mechanisms, Circ. Res. 114 (2014) 1453–1468.
[7] H. Cheng, M.B. Cannell, J.C. Hancox, Differential responses of rabbit ventricular and atrial transient outward current (Ito) to the Ito modulator NS5806, Phys. Rep. 5 (2017) e13172.
[8] Y. Pan, B. Li, J. Wang, X. Li, Rosuvastatin alleviates type 2 diabetic atrial structural and calcium channel remodeling, J. Cardiovasc. Pharmacol. 67 (2016) 57–67.
[9] C. Liu, H. Fu, J. Li, W. Yang, L. Cheng, T. Liu, et al., Hyperglycemia aggravates atrial interstitial fibrosis, ionic remodeling and vulnerability to atrial fibrillation in diabetic rabbits, Anadolu Kardiyol. Derg. 12 (2012) 543–550.
[10] T.F. Chao, K. Suenari, S.L. Chang, Y.J. Lin, L.W. Lo, Y.F. Hu, et al., Atrial substrate properties and outcome of catheter ablation in patients with paroxysmal atrial fibrillation associated with diabetes mellitus or impaired fasting glucose, J. Am. Coll. Cardiol. 106 (2011) 1615–1620.
[11] W.C. Claycombet, N.A. Lanson, B.S. Stallworth, et al., HL-1 cells: a cardiac muscle cell line that contracts and retains phenotypic characteristics of the adult cardiomyocyte, Proc. Natl. Acad. Sci. U.S.A. 95 (1998) 2979–2984.
[12] G.R. Norton, G. Candy, Aminoguanidine prevents the decreased myocardial compliance produced by streptozotocin-induced diabetes mellitus in rats, Circulation 93 (1996) 1905–1912.
[13] M. Brownlee, Biochemistry and molecular cell biology of diabetic complications, Nature 414 (2002) 813–820.
[14] X. Li, F. Rao, C.Y. Deng, et al., Involvement of ERK1/2 in Cx43 depression induced by macrophage migration inhibitory factor in atrial myocytes, Clin. Exp. Pharmacol. Physiol. 44 (2017) 771–778.
[15] F. Rao, C.Y. Deng, S.L. Wu, et al., Involvement of Src in L-type Ca^{2+} channel depression induced by macrophage migration inhibitory factor in atrial myocytes, J. Mol. Cell. Cardiol. 47 (2009) 586–594.
[16] J.P. Corsetti, J.D. Sparks, R.G. Peterson, R.L. Smith, C.E. Sparks, Effect of dietary fat on the development of non-insulin dependent diabetes mellitus in obese Zucker diabetic fatty male and female rats, Atherosclerosis 148 (2) (2000) 231–241.
[17] B. Wang, P.C. Chandrasekera, J.J. Pippin, Leptin- and leptin receptor-deficient rodent models: relevance for human type 2 diabetes, Curr. Diabetes Rev. 10 (2) (2014) 131–145.
[18] M.F. Pamarthi, M.A. Rudd, R.D. Bukoski, Normal perivascular sensory dilator nerve function in arteries of Zucker diabetic fatty rats, Am. J. Hypertens. 15 (4 Pt 1) (2000) 310–315.
[19] M. Watanabe, H. Yokoshiki, H. Mitsuyama, K. Mizukami, T. Ono, H. Tsutsui, Conduction and refractory disorders in the diabetic atrium, Am. J. Physiol. Heart Circ. Physiol. 303 (2012) H86–H95.
[20] T. Kato, T. Yamashita, A. Sekiguchi, K. Sagara, M. Takamura, S. Takata, et al., What are arrhythmogenic substrates in diabetic rat atria? J. Cardiovasc. Electrophysiol. 17 (2006) 890–894.
[21] C. Liu, R. Liu, H. Fu, J. Li, X. Wang, L. Cheng, et al., Pioglitazone attenuates atrial remodeling and vulnerability to atrial fibrillation in alloxan-induced diabetic rabbits, Cardiovascular therapeutics 35 (5) (2017).
[22] H. Fu, C. Liu, J. Li, C. Zhou, L. Cheng, T. Liu, et al., Impaired atrial electromechanical function and atrial fibrillation promotion in alloxan-induced diabetic rabbits, Cardiol. J. 20 (2013) 59–67.
[23] H. Fu, G. Li, C. Liu, J. Li, L. Cheng, W. Yang, et al., Probucol prevents atrial ion channel remodeling in an alloxan-induced diabetes rabbit model, Oncotarget 7 (2016) 83850–83858.
[24] X. Liu, S. Shi, H. Yang, C. Qu, Y. Chen, J. Liang, et al., The activation of N-methyl-d-aspartate receptors downregulates transient outward potassium and L-type calcium currents in rat models of depression, AJP Cell 313 (2017) C187–C196.
[25] H. Fu, G. Li, C. Liu, J. Li, X. Wang, L. Cheng, et al., Probucol prevents atrial remodeling by inhibiting oxidative stress and TNF-α/NF-κB/TGF-β signal transduction pathway in alloxan-induced diabetic rabbits, J. Cardiovasc. Electrophysiol. 26 (2) (2015) 211–222.
[26] D. Linz, M. Hohl, S. Dhein, S. Ruf, J.C. Reil, M. Kabiri, et al., Cathepsin A mediates susceptibility to atrial tachyarrhythmia and impairment of atrial emptying function in Zucker diabetic fatty rats, Cardiovasc. Res. 110 (3) (2016) 371–380.
[27] P. Pacher, Z. Ungvári, P.P. Nánási, V. Kecskeméti, Electrophysiological changes in rat ventricular and atrial myocardium at different stages of experimental diabetes, Acta Physiol. Scand. 166 (1999) 7–13.
[28] Y. Shimoni, L. Firek, D. Severson, W. Giles, Short-term diabetes alters K^+ currents in rat ventricular myocytes, Circ. Res. 74 (1994) 620–628.
[29] B. Yang, C. Li, J. Sun, X. Wang, X. Liu, C. Yang, et al., Inhibition of potassium currents is involved in antiarrhythmic effect of moderate ethanol on atrial fibrillation, Toxicol. Appl. Pharmacol. 322 (2017) 89–96.
[30] U. Schotten, S. Verheule, P. Kirchhof, A. Goette, Pathophysiological mechanisms of atrial fibrillation: a translational appraisal, Physiol. Rev. 91 (2011) 265–325.
[31] E.K. Johnson, S.J. Springer, W. Wang, E.J. Dranoff, Y. Zhang, E.M. Kanter, et al., Differential expression and remodeling of transient outward potassium currents in human left ventricles, Circ: Arrhythmia Electrophysiol 11 (2018) e005914.
[32] S.M. Schumacher, J.R. Martens, Ion channel trafficking: a new therapeutic horizon for atrial fibrillation, Heart Rhythm: the official journal of the Heart Rhythm Society 7 (9) (2010) 1309–1315.
[33] P. Cabanas-Grandío, F. Bisbal, E. Guiu, L. Mont, A. Berruezo, Deep breathing-triggered atrial fibrillation: an unusual mechanism terminated by focal RF ablation, Indian Pacing Electrophysiol. J. 15 (2015) 199–201.
[34] D.R. Van Wagoner, A.L. Pond, P.M. McCarthy, J.S. Trimmer, J.M. Nerbonne, Outward K^+ current densities and Kv1.5 expression are reduced in chronic human atrial fibrillation, Circ. Res. 80 (1999) 772–781.
[35] J. Tamargo, R. Caballero, R. Gómez, E. Delpón, $I_{(Kur)}$/Kv1.5 channel blockers for the treatment of atrial fibrillation, Expert Opin. Investig. Drugs 18 (2009) 399–416.
[36] M.C. Brandt, L. Priebe, T. Böhle, M. Südkamp, D.J. Beuckelmann, The ultrarapid and the transient outward K(+) current in human atrial fibrillation. Their possible role in postoperative atrial fibrillation, J. Mol. Cell. Cardiol. 32 (2000) 1885–1896.
[37] U. Ravens, C. Poulet, E. Wettwer, M. Knaut, Ultra-rapid delayed rectifier channels: molecular basis and therapeutic implications, Cardiovasc. Res. 89 (4) (2011) 776–785.
[38] Z. Lu, Y.P. Jiang, X.H. Xu, L.M. Ballou, I.S. Cohen, R.Z. Lin, Decreased l-type ca^{2+} current in cardiac myocytes of type 1 diabetic akita mice due to reduced phosphatidylinosItol 3-kinase signaling, Diabetes 56 (2007) 2780–2789.
[39] Z. Lu, L.M. Ballou, Y.P. Jiang, I.S. Cohen, R.Z. Lin, Restoration of defective l-type Ca^{2+} current in cardiac myocytes of type 2 diabetic db/db mice by akt and pkc-iota, J. Cardiovasc. Pharmacol. 58 (2011) 439–445.
[40] D. Li, S. Fareh, T.K. Leung, S. Nattel, Promotion of atrial fibrillation by heart failure in dogs: atrial remodeling of a different sort, Circulation 100 (1999) 87–95.